Postprint of:
CLAYS AND CLAY MINERALS Volume 67, Issue 2, 15 April 2019, Pages 173-182, 2019. **DOI:** 10.1007/s42860-019-00013-4

GRAFTED SEPIOLITES FOR THE REMOVAL OF PHARMACEUTICALS IN WATER TREATMENT

Tomás Undabeytia[1]*, Fernando Madrid[1], Juan Vázquez[2], and José Ignacio Pérez-Martínez[3]

1. Institute of Natural Resources and Agrobiology (IRNAS-CSIC). Reina Mercedes 10. Apdo. 1052. 41080 Sevilla. Spain.
2. Department of Organic Chemistry, University of Seville. Prof. García González 1, 41012 Seville, Spain.
3. Pharmacy and Pharmaceutical Technology Department, University of Seville. Prof. García González 2, 41012 Seville, Spain.

[*Received 19 December 2017; revised 26 December 2018; Ms. 1251; AE: G. Rytwo*]
Footnote: This paper was originally presented during the session NT-06: Clays, organo-clays, and nanocomposites in water treatment during ICC 2017.

Running head: Grafted sepiolites for the removal of pharmaceuticals

*E-mail: undabeyt@irnase.csic.es

Abstract

The increased detection of pharmaceuticals in finished drinking water has become a growing cause of concern in recent years. The removal of atenolol, ranitidine, and carbamazepine by sepiolite, following functionalization of its surface by organosilane grafting, constituted the subject of this investigation. Silylated surfaces include octyl, γ-aminopropyl, 3-chloropropyl, and triphenyl moieties. The sorption of atenolol and ranitidine was higher on sepiolite functionalized with 3-chloropropyl, while carbamazepine showed a higher sorption on sepiolite with triphenyl groups. Filtration experiments of both ranitidine and carbamazepine on octyl- and triphenyl-sepiolite, respectively, showed a higher retention of ranitidine in comparison to carbamazepine, in spite of the fact that the number of sorption sites was lower due to its higher binding rate.

Key words: Filtration, Grafting, Pharmaceuticals, Sepiolite, Sorption.

INTRODUCTION

In recent years, organic microcontaminants in surface waters have been detected frequently. These emerging contaminants (ECs) comprise a great variety of chemicals such as pharmaceuticals (PhAcs), personal care products, surfactants, steroid hormones, plasticizers, fire retardants, pesticides, *etc*. (Hedgespeth *et al*., 2012; Luo *et al*, 2014). Several recent reviews have confirmed the presence of ECs in finished drinking waters across the world, as treatment processes largely fail to reduce the amounts of these substances to below current detection limits (Kleywegt *et al*., 2011; Rodil *et al*., 2012; Meffe and Bustamante, 2014).

Granular activated carbon (GAC) is used in the majority of water treatment plants. A good correlation between the percentage removal by activated carbon and the octanol/water partition coefficient (Kow) has been found, however, only for compounds with log Kow > 3 (Zwiener, 2007). Studies, therefore, now focus on the search for alternative or complementary sorbents to improve EC removal. In this context, clay minerals, as sorbents with unique properties such as large surface area, low cost, and high abundance, have been assessed for the removal of ECs after functionalizing their surfaces for improved performance. This is achieved usually by two methods: cationic exchange reactions and grafting of organic groups. The most widely used cations for intercalation on the clay surface are quaternary ammonium surfactants and polymers (Gardi *et al*., 2015; Shabtai and Mishael, 2016). Lelario *et al.* (2017) studied the removal of three ECs by laboratory-scale filtration using three clay-based composites prepared from two cationic surfactants and one polycation. The removal was strongly dependent on the modifier used, which affected the interaction mechanism. However, potential leaching of the modifier during water treatment represents a considerable concern and needs to be addressed. One potential approach may involve silane grafting

(silylation) of the clay mineral surfaces, which provides a durable immobilization of the modifier by covalent bonding (polycondensation) between the organosilane agents and the OH of the clay surfaces (He *et al*., 2013). The adsorption selectivity of the silylated surface can be improved by introducing specific functional reactant groups. Based on previous studies, amino- or mercapto-grafted clays are effective sorbents for the removal of heavy metals by chelation (Tonle *et al*., 2003; Liang *et al*., 2014). Silylated clays have also demonstrated a high level of efficacy for the removal of organic pollutants (Paul *et al.*, 2011a). Studies regarding the use of grafted sepiolites in the removal of organic pollutants, however, are scarce (Paul *et al*., 2011b).

In the current study, the removal of three PhAcs *via* a commercially available sepiolite and following the silylation of its surface was studied. The specific objectives were: (i) to modify the sepiolite surface by grafting onto its external surface organic moieties that render it with different physicochemical properties; (ii) to study the removal of PhAcs as a function of their nature and of the grafted groups; and (iii) to test the new materials for their potential use in filtration processes.

MATERIALS AND METHODS

Materials

Sepiolite (Pangel S9) was obtained from Tolsa S.A. (Madrid, Spain). Pangel S9 is a high purity sepiolite produced after selection in the mine followed by a wet micronization process that permits the removal of the large amount of higher density impurities such as feldspars, quartz, carbonates, and other detrital materials. Its X-ray diffraction pattern corresponds to sepiolite (Figure 1). Its physical appearance is a fluid, creamy-colored powder; its specific surface is 320 m^2/g; and it has a cationic exchange capacity of 0.15 $mmol_c/g$.

92 Analytical-grade organosilane agents and pharmaceuticals were obtained from Sigma-
93 Aldrich (Sigma Chemical Co., St Louis, Missouri, USA). The organosilane grafting
94 agents were γ-aminopropyltriethoxysilane (APTES), 3-chloropropyltriethoxysilane
95 (CPTES), triethoxy(octyl)silane (OTES), and phenyltrichlorosilane (TFS). The
96 pharmaceuticals studied were atenolol, carbamazepine, and ranitidine (Figure 2).
97 Granular activated carbon (NUSORB GC60, 12×30 mesh) was purchased from
98 NUCON International, Inc. (Columbus, Ohio, USA); High Performance Liquid
99 Chromatography (HPLC)-grade acetonitrile and methanol were obtained from
100 Teknokroma S.A. (Barcelona, Spain).
101
102 *Preparation of grafted sepiolites*
103 One gram of pristine sepiolite was refluxed for 24 h in 50 mL of dry toluene with an
104 amount of organosilane equivalent to the amount of silanol groups on the clay surface
105 (0.6 mmol) (Rytwo *et al.*, 1998). The reaction was carried out in an oxygen-free
106 environment. Having completed the reaction, the mixture was filtered and washed with
107 50 mL of anhydrous ethanol and the product was dried at 60ºC for another 24 h. The
108 amount of grafted organosilane was determined by elemental C analysis (LECO
109 Elemental Analyzer, model CHNS 932). Parallel experiments were performed using
110 twice the amount of organosilane. The grafted sepiolites are abbreviated as Y-sep,
111 where Y refers to the organosilane agent.
112
113 *Preparation of sorption-based sepiolites*
114 Sorption of the organosilane agents on the clay was performed in toluene at a clay
115 concentration of 1.6 g/L. The organosilane was added at 5-fold the concentration of

116 silanol groups. After shaking for 24 h, the suspension was centrifuged for 15 min at
117 39200 g, and the pellets were lyophilized.
118
119 *Characterization of functionalized sepiolites*
120 Thermogravimetric analysis (TG) and deffertial thermogravimetry (DTG) analysis of
121 the samples were performed using a modulated SDT Q600 system and the software
122 package *Universal Analysis-NT 2000* (TA-Instruments, New Castle, Delaware, USA).
123 The samples (2–6 mg) were heated at a rate of 10ºC/min from 30 to 1100ºC in
124 aluminum pans with a pin hole under a nitrogen atmosphere (60 mL/min).
125 Fourier-transform infrared (FTIR) spectra were recorded from KBr pellets (2 wt.%
126 sample), using a 6100 Jasco spectrometer (Easton, Maryland, USA) with a DTGS
127 detector, in the range 4000–400 cm^{-1} and with a resolution of 2 cm^{-1}. In order to
128 improve the signal-to-noise ratio in the spectra, 300 scans were undertaken.
129 Zeta potential measurements of suspensions of the organo-sepiolites following
130 redispersion at a concentration of 1.6 g/L were performed using a Zetasizer Nanosystem
131 (Malvern Instruments, Southborough, Massachusetts, USA). The samples were allowed
132 to equilibrate for 1 h before a several mL aliquot of the dispersion was analyzed. The
133 temperature of the samples was 25±1ºC. The zeta potential was deduced from the
134 mobility of the particles using the Smoluchowski equation.
135
136 *Sorption experiments*
137 Sorption isotherms of ranitidine, atenolol, and carbamazepine onto sepiolite and grafted
138 sepiolites were conducted in triplicate by mixing 15 mL of the solutions of each
139 adsorbate (0–50 mg/L) with 24 mg of clay; clay concentration was 1.6 g/L. Having been

shaken for 24 h at 20ºC, the suspensions were centrifuged at 12,000×g for 10 min, and the analyte in the supernatants was measured *via* HPLC.

Sorption was modeled by using the Langmuir-Scatchard equation:

$$\frac{Lo-L}{L} = \frac{Ro * K_L}{1+K_L * L} \qquad (1)$$

where Lo and L denote the molar concentration of total and free surfactant, respectively, Ro is the molar concentration of sorption sites, and K_L is the binding coefficient.

Removal of PhAcs by filtration

Column filter experiments were performed using a 50/1 (w/w) mixture of quartz sand with grafted clay ~~or with GAC~~. Glass columns with a length of 21 cm and a diameter of 2 cm, containing a porous plate at the bottom, were filled with 73.5 g of thin quartz sand mixed with 1.5 g of clay-polymer complexes (Experiment 1). The active sorbent layer was 13 cm thick. Glass wool (0.35 g) was placed on both ends of the column to prevent sand loss. The pore volume of the column was 12.9 mL and it was connected to a peristaltic pump and saturated at a constant flow rate of 10 mL/min with distilled water. Single solutions of PhAcs at a concentration of 5 mg/L were passed through the columns.

Different constructive and operational parameters were used in another filtration experiment (Experiment 2), with columns 24 cm long and 3 cm in diameter and filled with 154 g of sand and 3.1 g of composite. The pore volume was 38 mL and the sorbent layer was 10 cm thick. A 1 mg/L solution of PhAcs was filtered at a flow rate of 12 mL/min.

Analysis of the kinetics of filtration.

In this analysis, the adsorption and convection phenomena occurring in the filter were described by equation 2 as in Nir *et al*. (2012). A column of length *L* was filled with material whose initial molar concentration of adsorbing sites was *R*o, and whose concentration later changed to *R*(X,t). The beginning and end of the filter were at the coordinates X = 0 and X = *L*, respectively. The pollutant concentration at the inlet, *C*o, was constant, *i.e*. *C*(X,t) = *C*o, X ≤ 0, where t denotes time.

The kinetics parameters were *C*1 (M^{-1} min^{-1}, rate constant of forward adsorption), D1 (min^{-1}, rate constant of desorption), and *v* (flow velocity). The equation used was:

$$\frac{dC(X,t)}{dt} = -v\,\frac{\partial C}{\partial X} - [C1 \cdot C(X,t) \cdot R(X,t)] + \left[D1 \cdot \left(R_0 - R(X,t)\right)\right] \qquad (2)$$

The statistical criteria employed for simulation and prediction of certain experimental results of filtration by the calculations according to equation 2 were the values of R^2.

Analysis of pollutants

The solutions were analyzed isocratically using a Shimadzu HPLC (Kyoto, Japan) equipped with a photo diode array detector. The reverse-phase column used was a 15-cm Kromasil 100 C18, with a flow rate of 1.0 mL/min. The mobile phases were binary mixtures of (1) methanol with water acidified to pH 3.0 by glacial acetic acid at a ratio of 45:55 for atenolol, of (2) methanol with 0.5 M ammonium acetate at a ratio of 20:80 for ranitidine, and of (3) acetonitrile with 10 mM of KH_2PO_4 acidified to pH 2.5 with phosphoric acid at a ratio of 30:70 for carbamazepine. The PhAcs concentrations were measured at the following wavelengths: atenolol at 230 nm, ranitidine at 254 nm, and carbamazepine at 210 nm. The retention times were 2.55 min for atenolol, 4.20 min for ranitidine, and 4.94 min for carbamazepine.

RESULTS AND DISCUSSION

189 ***Characterization of functionalized sepiolites***

190 Organosilane covalently bonded to sepiolite can be obtained through one, two, or three
191 silanols on the sepiolite surface. Moreover, additional polymerization between the
192 grafted organosilanes may occur. Elemental C analysis of the grafted sepiolites enabled
193 determination of the reaction products (Table 1). On APTES-sep, CPTES-sep, and
194 OTES-sep, the amount of organosilane grafted did not change with increasing amounts
195 of added organosilane. The amount of grafted APTES on sepiolite indicated that each
196 molecule reacted with one silanol. The excess of organosilane, over the amount of
197 silanol groups on the sepiolite surface, may interact with other mineral phases present
198 (the mineral used accounted for 85% of sepiolite) or within the channels by cationic
199 exchange through protonation of the amine moieties. Unlike APTES, the amount of
200 grafted CPTES-sep was relatively close to that of the silanol groups; hence, one CPTES
201 molecule reacted with one silanol on the sepiolite surface. In contrast, the small amount
202 of grafted organosilane on OTES-sep showed that each OTES molecule reacted with
203 three silanols on the sepiolite surface, yielding a value of grafted silanols of
204 0.54 mmol/g, which is relatively close to the total amount of silanols on the sepiolite
205 surface (0.6 mmol/g). The high loading of TFS after grafting is proof of polymerization
206 between TFS molecules. The adsorbed surface water of sepiolite provoked hydrolysis of
207 Si–Cl bonds to form Si–OH groups, forming a tridimensional network by
208 polycondensation reactions. Limiting factors are the amount of organosilane and water
209 in the system (Fadeev and ~~&~~ McCarthy, 2000; Fadeev and Kazakevich, 2002).
210 The surface charge of the sepiolite after silanization with the organosilane agents was
211 determined by zeta potential measurements. The isoelectric point (IEP) of this sepiolite
212 is 2.7 (Jalali *et al*., 2016), and so its surface was negative at the pH of the suspension.
213 After grafting with the organosilanes with the exception of APTES, the surface

potentials were more negative and similar which was not related to the pH of the suspensions given their more acidic character. The absence of variable charges due to silanols located on the external surface of the sepiolite and providing certain positive charges enhanced the permanent negative charges associated with isomorphic substitutions. This sepiolite has 0.17–0.23 Al atoms every 12 tetrahedral positions (García-Romero and Suárez, 2010) inducing a polarized charge on the basal oxygens of the external tetrahedral planes, enabling them to behave as weak electron donors. When the surface of the clay was grafted with APTES, the surface potential was reversed due to the excess of positive charge of the amine moieties protonated at the pH of the suspension.

After grafting with the organosilane agents, the TG-DTG curves of pristine sepiolite (Figure 3) showed four mass losses due to: a) removal of adsorbed water up to 100ºC (weight loss of 8.0%); b) removal of zeolitic water up to 270ºC (3.2% weight loss); c) removal of water coordinated to Mg ions up to 600ºC (2.5% weight loss); and d) dehydroxylation followed by folding of the structure up to 1,000ºC (2.1% weight loss) (Frost and Ding, 2003; Post *et al*., 2007). The TG-DTG curves of the complexes prepared by sorption of the organosilanes were fairly similar to those of pristine sepiolite (data not shown), in contrast to those obtained from the grafted sepiolites. After APTES grafting, a weight loss of 3.0% was observed between the losses of adsorbed and zeolitic water. This loss is closely related to the decomposition of liquid APTES (157ºC), revealing the presence and degradation of loosely bound molecules of the organosilane agent. The loss of zeolitic water also occurred over a broader temperature range, most likely due to the increased polarization of certain water molecules after interacting with amine moieties of APTES. The largest loss (13.2%) occurred between 300 and 600ºC and was associated mainly with the decomposition of

239 grafted APTES molecules. The TG-DTG pattern of OTES-sep was completely different
240 from those of the other modified sepiolites. A significant loss of weight in the 270–
241 600ºC range (~14%) was observed, which was considerably larger than that associated
242 with water chemically bound to Mg^{2+} ions (2.5%). In the DTG, a sharp peak at 532ºC
243 was noticed for the OTES-sep only, confirming a uniform reaction on the sepiolite
244 surface, as previously mentioned. In contrast, the TFS-sep yielded on the DTG curve
245 overlapped several peaks between 300 and 800ºC, which indicates several TFS
246 interaction mechanisms, covalently bound to the sepiolite surface and in-between the
247 grafted TFS molecules as well as to the formation of the char. The DTG of CPTES-sep
248 showed a peak at approx. 370ºC, which was not detected in sepiolite, associated with
249 the decomposition of the grafted CPTES.
250 The FTIR spectrum of sepiolite shows bands at 3692 and 3634 cm^{-1} (Figure 4), ascribed
251 to vibrations of OH groups in the octahedral sheet (Mg_3OH) and in the external surface
252 (Si–OH stretch). The zeolitic water and the water bound to Mg in the octahedral sheet
253 were responsible for the vibrations at 3558, 3405, 3233, and 1664–cm^{-1} (Alkan *et al.*,
254 2005). The tetrahedral sheet yielded absorption bands at 1211, 1084, and 969–cm^{-1},
255 associated with the Si–O stretch (Frost *et al*., 2001).
256 The APTES-sep showed absorption bands at 1562 and 1492 cm^{-1} due to the bending
257 vibrations of the $–NH_2$ and $–CH_2$ groups. Other absorptions were at 2933–cm^{-1} and a
258 shoulder at 2869–cm^{-1}, associated with the asymmetric and symmetric stretching of CH_2
259 groups. When OTES and CPTES were grafted, the most relevant features were the
260 presence of absorption bands at 2958 cm^{-1} due to CH_3 and at 2933 and 2856 cm^{-1} due to
261 the asymmetric and symmetric stretch of CH_2 groups. In the case of OTES in particular,
262 the increased hydrophobicity following silanization modified water vibrations, as
263 reflected in the doublet observed at 1702 and 1664 cm^{-1}, associated with O–H water

264 bending vibrations. In the TFS-sep, the skeletal ring-breathing modes of phenyl
265 moieties were observed at 1588 and 1428 cm^{-1}. The FTIR data confirmed the interaction
266 of the organosilane agents with the sepiolite surface. No additional absorption bands to
267 those of pristine sepiolite were recorded for modified sepiolites based on the sorption of
268 the organosilane agents, probably owing to their low affinity (data not shown).
269
270 ***Sorption studies***
271 The sorption of PhAcs was strongly dependent on the organosilane grafted on the
272 surface of sepiolite, and their speciation was related to the equilibrium pH (Figure 5).
273 The pH ranged between 6.7 and 8.5 for carbamazepine, 5.6 to 8.3 for ranitidine, and 6.7
274 to 7.3 for atenolol, with the exception of the sorption of the three PhAcs on APTES-sep
275 (pH 9.1–9.7). Atenolol sorption was greater on CPTES- and OTES-sepiolites,
276 presenting isotherms of extremely high affinity (H-type). Its sorption was moderate on
277 sepiolite and TFS-sep with isotherms of L-type, whereas the least sorption occurred on
278 APTES-sep. Atenolol remained in the solution as a cation (pKa = 9.6), which explains
279 its high sorption on sepiolite *via* a cationic exchange mechanism. TFS grafting did not
280 significantly affect this mechanism. The covering of the surface with TFS molecules
281 increases its hydrophobicity, restricting sorption by cationic exchange to a certain
282 degree; however, a certain fraction of atenolol may be sorbed by π–π^* interactions
283 between the phenyl rings of TFS molecules and of the drug. Modification of the
284 sepiolite surface with OTES and CPTES increased the affinity, but different modes of
285 interaction operated. With the OTES-sep, the increased hydrophobicity of the surface by
286 grafting alkyl chains facilitated the interactions with the lyophobic moieties of atenolol.
287 Greater sorption was expected on CPTES-sep than on OTES-sep, based on the
288 formation of donor-acceptor complexes between Cl and the protonated amine of

289 atenolol as well as owing to the aromatic ring of this molecule, as described for the
290 polar molecule imazaquin (Paul *et al*., 2011b). The similar sorption of atenolol on these
291 two sorbents reflects the formation of a near-partition phase through interaction of the
292 grafted alkyl chains with a high affinity to atenolol, albeit the alkyl chains were slightly
293 smaller than those described for its formation (C_{10}).
294 In the case of APTES-sep, the sorption isotherm followed the C-type, which is typical
295 of a partition mechanism. The organic modifier remained mostly as a cation (~93%) at
296 the equilibrium pH (9.7), whereas a significant fraction of atenolol was neutral (~50%).
297 Some of these neutral molecules interacted with the $–NH_3^+$ of the APTES. This pattern
298 was also reflected in the sorption of the other PhAcs on APTES-sep. This surface
299 always recorded the least amounts sorbed.
300 Ranitidine sorption also followed the H-type on CPTES- and OTES-sepiolites as well as
301 on pristine sepiolite, indicating a preferential cationic exchange mechanism for its
302 sorption. Additional hydrophobic interactions were responsible for enhanced sorption
303 on OTES-sep, whereas the greatest sorption was observed for CPTES-sep. Unlike
304 atenolol, the sorption of ranitidine on TFS-sep was poor. In contrast, carbamazepine
305 showed the highest sorption on TFS-sep. Hydrophobic interactions were clearly
306 responsible for its sorption on the grafted sepiolites. The order of affinity followed the
307 increase in hydrophobicity: TFS-sep > OTES-sep > CPTES-sep > sep > APTES-sep.
308 The largest sorption of carbamazepine was on TFS-sep due to the greater number of π–
309 π* interactions between the aromatic rings of the drug and those of phenyl grafted on
310 the sepiolite surface, similar to those reported for the sorption of non-polar aromatic
311 molecules on clay minerals supporting benzyl- and phenyl-moieties (Nir *et al*., 2000).
312 The sorption isotherms were fitted to the Langmguir-Scatchard equation (equation 1).
313 As in Galán-Jiménez *et al*. (2013), only one fitting parameter was used in the modeling,

314 the binding coefficient K_L. In the determination of the binding coefficients, the
315 concentration of sorption sites (R_0) was fixed for each composite (Table 1). A high level
316 of agreement was observed between the experimental and the calculated sorbed
317 amounts of PhAcs (Table 2). The regression coefficients were >0.90, with the exception
318 of atenolol and ranitidine sorbed on TFS-sep and APTES-sep, respectively.
319 The largest K_L values determined were of the order of magnitude found for the removal
320 of PhAcs by other sorbents. Polubesova *et al*. (2006) reported values between 7000 and
321 20,000 M^{-1} for the sorption of tetracyclines and sulfonamides on a micelle-clay
322 complex. Using a different clay-micelle complex, Karaman *et al*. (2012) obtained a K_L
323 value of 21,000 M^{-1} for the removal of diclofenac. The great affinity of the PhAcs for
324 these micelle-clay complexes was explained by their excess of positive charge binding
325 the negatively charged molecules of the PhAcs. With grafted sepiolites, the electrostatic
326 interactions were not primarily responsible for the retention of PhAcs as noted in the
327 two- to six-fold increase in the K_L values of ranitidine and atenolol for certain modified
328 clays relative to sepiolite. Recently, Lozano-Morales *et al*. (2018) reported larger
329 affinity of atenolol by polymer-clay composites based on cationic starches (K_L: 20,000–
330 80,000 M^{-1}).
331
332 ***Filtration experiments***
333 Modification of the sepiolite's surface was necessary for its use in filtration experiments
334 in order to preclude the formation of a gel that would clog the filter. In the first stage,
335 the filtration experiments of single solutions of the three PhAcs were conducted using a
336 combination of OTES-sep and TFS-sep as part of the filtering medium. According to
337 the K_L values, the highest sorption affinity of the three PhAcs was found for OTES-sep,
338 but the sequence of the sorption (Figure 5) showed a greater affinity of ranitidine on

339 CPTES-sep and of carbamazepine on TFS-sep. This apparent contradiction can be
340 explained by the presence of a larger number of sorption sites (*R*o), albeit with lower
341 affinity for the PhAcs than for OTES-sep. This lower affinity for the modified sepiolite
342 surfaces was overcome by the greater number of sorption sites, resulting in a greater
343 sorption of the drugs than on OTES-sep. Therefore, the selection of the combination of
344 OTES-sep and TFS-sep represented a compromise between an adsorbent with a
345 considerable affinity for PhAcs and an adsorbent with lower affinity but a larger number
346 of sorption sites. The breakthrough curves revealed very poor levels of performance in
347 the retention of the PhAcs by the filters (Figure 6). This was slightly improved by the
348 removal of carbamazepine, whereas similar curves were obtained for ranitidine and
349 atenolol. Therefore, any improvement in the retention in the filters was tested for
350 ranitidine and carbamazepine using OTES-sep and TFS-sep, respectively, *i.e*. the use of
351 the medium with particularly large affinity for each PhAcs. Atenolol was circumvented
352 due to its similar pattern to ranitidine.
353 The pattern in the elution curves of ranitidine and carbamazepine changed drastically by
354 using only one of the complexes (Figure 7a). Ranitidine did not elute in the first 60 pore
355 volumes, whereas no elution was seen for carbamazepine during the first 25 pore
356 volumes. The efficiency was clearly better for ranitidine, which did not reach 50% of
357 the amount applied until the seepage of 80 pore volumes, in contrast with a value of 50
358 pore volumes for carbamazepine, in agreement with the magnitude of K_L values.
359 The filtration of the PhAcs was modeled using the filtration kinetics model (equation 2);
360 the fitting was adequate (Table 3, Figure 7a). An estimation of the binding rates (K =
361 $C1/D1$) yielded a value of 611 M^{-1} for carbamazepine and 4166 M^{-1} for ranitidine, that
362 is, the least eluted fraction expected for ranitidine as observed experimentally, which
363 also followed the trend in K_L values.

364 The goodness of the model was examined for its predictive character under other
365 conditions than those used in the determination of the fitting parameters. In a parallel
366 experiment, the removal of ranitidine and carbamazepine was studied under different
367 operational conditions (2.25 times the filter diameter; twice the sorbent concentration;
368 1.6-fold the flow velocity) (Figure 7b). The removal was very efficient for ranitidine
369 which did not show any elution during the first 114 pore volumes whereas a minute
370 amount was detected for carbamazepine after 28 pore volumes. The model again
371 performed rather well for ranitidine ($R^2 = 0.95$) and carbamazepine ($R^2 = 0.87$), and
372 fitted particularly well in the regime of low pore volume numbers, which is of prime
373 interest in order to determine the amount of water capable of being produced by the
374 system, fulfilling the legal requirements for water purification. Consequently, the model
375 can be employed to predict the eluted amounts for other scenarios, especially for the
376 determination of the elution at low pollutant concentrations.
377
378 **CONCLUSIONS**
379 The removal of three PhAcs was studied *via* sepiolite, the surface of which was
380 modified by grafting organosilanes to avoid leaching of the modifier during sorption
381 and filtration. The study of the anchored amounts of the organosilanes and the thermal
382 and infrared analysis of the grafted sepiolites confirmed different mechanisms of
383 interaction with the sepiolite surface. Sorption studies revealed specific interactions
384 between grafted moieties and the PhAcs: π–π^* interactions between phenyl rings,
385 donor-acceptor complexes between electronegative atoms and protonated groups, as
386 well as hydrophobic interactions between alkyl chains. Therefore, certain PhAcs can be
387 immobilized by the use of tailored adsorbents, focusing on their structure and
388 compatibility with the grafted moieties.

389 Most studies of sorbents in filtration have focused on the immobilization of anionic and
390 neutral PhAcs, which is true of most of the pharmaceuticals found in surface waters.
391 However, their performance was usually poor when removing pollutants with a certain
392 cationic character. The use of grafted sepiolites represents an effective alternative,
393 which in combination with other sorbents may broaden the removal of PhAcs and
394 increase the amount of water purified.
395
396 **ACKNOWLEDGMENTS**
397 This research was supported by the MEC projects CTM2013-42306-R and CTM2016-
398 77168-R. Both projects received funding from the European Social Fund. The authors
399 acknowledge the CITIUS service from the University of Seville for thermal analysis
400 facilities. The authors also thank Prof. Shlomo Nir for his assistance in modeling the
401 filtration data.
402
403
404 **REFERENCES**
405 Alkan, M., Tekin, G. and Namli, H. (2005). FTIR and zeta potential measurements of
406 sepiolite treated with some organosilanes. *Microporous and Mesoporous Materials,* **84**,
407 75-83.
408
409 Fadeev, A. and McCarthy, T.J. (2000). Self-assembly is not the only reaction possible
410 between alkyltrichlorosilanes and surfaces: Monomolecular and oligomeric covalently
411 attached layers of dichloro- and trichloroalkylsilanes on silicon. *Langmuir,* **16,** 7268-
412 7274.
413

414 Fadeev, A. and Kazakevich, Y.V. (2002). Covalently attached monolayers of oligo
415 (dimethylsiloxane)s on silica: A siloxane chemistry approach for surface modifications.
416 *Langmuir,* **18**, 2665-2672.
417
418 Frost, R.L. and Ding, Z. (2003). Controlled rate thermal analysis and differential
419 scanning calorimetry of sepiolites and palygorskites. *Thermochimica Acta*, **397**, 119-
420 128.
421
422 Frost, R.L., Locos, O.B., Ruan, H. and Kloprogge, T. (2001). Near-infrared and mid-
423 infrared spectroscopic study of sepiolites and palygorskites. *Vibrational Spectroscopy,*
424 **27**, 1-13.
425
426 García-Romero, E. and Suárez, M. (2010). On the chemical composition of sepiolite
427 and palygorskite. *Clays and Clay Minerals,* **58**, 1-20.
428
429 Gardi, I., Nir, S. and Mishael, Y.G. (2015). Filtration of triazine herbicides by polymer-
430 clay sorbents: Coupling an experimental mechanistic approach with empirical
431 modeling. *Water Research,* **70**, 64-73.
432
433 He, H., Tao, Q., Zhu, J., Yuan, P., Shen, W. and Yang, S. (2013). Silylation of clay
434 mineral surfaces. *Applied Clay Science,* **71**, 15-20.
435
436 Hedgespeth, M., Sapozhnikova, Y., Pennington, P., Clum, A., Fairey, A. and Wirth, E.
437 (2012). Pharmaceuticals and personal care products (PPCPs) in treated wastewater

438 discharges into Charleston Harbor, South Carolina. *Science of the Total Environment,*
439 **437**, 1-9
440
441 Jalali, A.M. Taromi, F.A., Atai, M. and Solhi, L. (2016). Effect of reaction conditions
442 on silanisation of sepiolite nanoparticles. *Journal of Experimental Nanoscience,* **15**,
443 1171-1183.
444
445 Karaman, R, Khamis, M., Quried, M.; Halabieh, R., Makharzeh, I., Manassra, A,
446 Abbadi, J., Qtait, A., Bufo, S.A., Nasser, A. and Nir, S. (2012). *Environmental*
447 *Technology,* **33**, 1279-1287.
448
449 Kleywegt, S., Pileggi, V., Yang, P., Hao, C., Zhao, X., Rocks, C., Thach, S., Cheung, P.
450 and Whitehead, B. (2011). Pharmaceuticals, hormones and bisphenol A in untreated
451 source and finished drinking water in Ontario, Canada-occurrence and treatment
452 efficiency. *Science of the Total Environment,* **409**, 1481-1488.
453
454 Lelario, F., Gardi, I., Mishael, Y.G., Dolev, N., Undabeytia, T., Nir, S., Scrano, L. and
455 Bufo, S.A. (2017). Pairing micropollutants and clay-composite sorbents for efficient
456 water treatment: Filtration and modeling at pilot scale. *Applied Clay Science,* **137**, 225-
457 232.
458
459 Liang, X., Xu, Y., Sun, G., Wang, L., Sun, Y., Sun, Y. and Qjn, X. (2011). Preparation
460 and characterization of mercapto functionalized sepiolite and their application for
461 sorption of lead and cadmium. *Chemical Engineering Journal,* **174**, 436-444.
462

463 Lozano-Morales, V., Gardi, I., Nir, S. and Undabeytia, T. (2018). Removal of
464 pharmaceuticals from water by clay-cationic starch sorbents. *Journal of Cleaner*
465 *Production,* **190**, 703-711.
466
467 Luo, Y., Guo, W., Ngo, H.H., Nghiem, L.D., Hai, F.I., Zhang, J., Liang, S. and Wang,
468 X.C. (2014). A review on the occurrence of micropollutants in the aquatic environment
469 and their fate and removal during wastewater treatment. *Science of the Total*
470 *Environment,* **473-474**, 619-641.
471
472 Meffe, R. and Bustamante, I. de. (2014). Emerging organic contaminants in surface
473 water and groundwater: A first overview of the situation in Italy. *Science of the Total*
474 *Environment,* **481**, 280-295.
475
476 Nir, S., Undabeytia, T., Yaron-Marcovich, D., El-Nahhal, Y., Polubesova, T., Serban,
477 C., Rytwo, G., Lagaly, G. and Rubin, B. (2000). Optimization of adsorption of
478 hydrophobic herbicides on montmorillonite preadsorbed by monovalent organic cations:
479 Interaction between phenyl rings. *Environmental Science and Technology,* **34**, 1269-
480 1274.
481
482 Paul, B., Martens, W.N. and Frost, R.L. (2011a). Organosilane grafted acid-activated
483 beidellite clay for the removal of non-ionic alachlor and anionic imazaquin. *Applied*
484 *Surface Science,* **257**, 5552-5558.
485

Paul, B., Martens, W.N. and Frost, R.L. (2011b). Surface modification of alumina nanofibers for the selective adsorption of alachlor and imazaquin herbicides. *Journal of Colloid and Interface Science,* **360**, 132-138.

Polubesova, T., Zadaka, D., Groisman, L. and Nir, S. (2006). Water remediation by micelle-clay system: Case study for tetracycline and sulfonamide antibiotics. *Water Research,* **40**, 2369-2374.

Rodil, R., Quintana, J.B., Concha-Graña, E., López-Mahía, P., Muniategui-Lorenzo, S. and Prada-Rodríguez, D. (2012). Emerging pollutants in sewage, surface and drinking water in Galicia (NW Spain). *Chemosphere,* **86**, 1040-1049.

Rytwo, G., Nir, S., Margulies, L., Casal, B., Merino, J., Ruiz-Hitzky, E. and Serratosa, J.M. (1998). Adsorption of monovalent organic cations on sepiolite: Experimental results and model calculations. *Clays and Clay Minerals* **46**, 340-348.

Shabtai, I.A. and Mishael, Y.G. (2016). Efficient filtration of effluent organic matter by polycation-clay composite sorbents: Effect of polycation configuration on pharmaceutical removal. *Environmental Science and Technology,* **50**, 8246-8254.

Tonle, I.K., Ngameni, E., Njopwouo, D., Carteret, C. and Walcarius, A. (2003). Functionalization of natural smectite-type clays by grafting with organosilanes: physic-chemical characterization and application to mercury (II) uptake. *Physical Chemistry Chemical Physics,* **5**, 4951-4961.

511 Zwiener, C. (2007). Occurrence and analysis of pharmaceuticals and their
512 transformation products in drinking water treatment. *Analytical and Bioanalytical*
513 *Chemistry,* **387**, 1159-1162.
514

515 **TABLE 1.** Zeta potential of sepiolite and organo-sepiolites and the amounts of

516 organosilane grafted on sepiolite.

	Zeta potential (mV)[a]	Concentration (mmol/g)
Sepiolite	–7.28±0.48 (7.4)	-
APTES-sep	8.97±0.28 (8.2)	1.05±0.10
CPTES-sep	–15.70±2.47 (6.0)	0.44±0.02
OTES-sep	–14.55±0.51 (6.3)	0.17±0.01
TFS-sep	–16,63±1.71 (5.6)	2.20±0.20

517 a. The pH values of the organo-sepiolite suspensions are provided in parentheses.

518

519 **TABLE 2.** K_L values and R^2 from the fit of the experimental sorption values to the

520 Langmuir equation.

Atenolol		
Sorbent	K_L (M^{-1})	R^2
Sepiolite	800	0.92
APTES-sep	75	0.92
CPTES-sep	1650	0.94
OTES-sep	5000	0.95
TFS-sep	250	0.85
Carbamazepine		
Sorbent	K_L (M^{-1})	R^2
Sepiolite	200	0.95
APTES-sep	50	0.97
CPTES-sep	2200	0.92
OTES-sep	2800	0.99
TFS-sep	700	0.99
Ranitidine		
Sorbent	K_L (M^{-1})	R^2
Sepiolite	1800	0.96
APTES-sep	85	0.85
CPTES-sep	5400	0.99
OTES-sep	10500	0.98
TFS-sep	150	0.93

521

522

523 TABLE 3. Calculated coefficients and R^2 of the fit of the experimental data to the
524 adsorption and convection model (equation 2).

	*R*o (M)	*C*1 (M^{-1} min^{-1})	*D*1 (min^{-1})	R^2
Ranitidine	0.026	750	0.18	0.98
Carbamazepine	0.035	550	0.90	0.93

525

526

FIGURE CAPTIONS

FIGURE 1. XRD pattern of the sepiolite Pangel S9.

FIGURE 2. Structural formula of PhAcs.

FIGURE 3. TG-DTG curves of sepiolite and following the grafting of its surface with organosilane agents.

FIGURE 4. FTIR spectra of sepiolite and organo-sepiolites.

FIGURE 5. Sorption isotherms on sepiolite and organo-sepiolites of atenolol, ranitidine, and carbamazepine.

FIGURE 6. Eluted percentages of atenolol, ranitidine, and carbamazepine in filtration experiments including GAC or grafted sepiolites (OTES- and TFS-sepiolites) mixed with sand (1:50 w/w). The concentration of the PhAcs in the solution was 5 mg/L.

FIGURE 7. Experimental and theoretical elution curves of ranitidine and carbamazepine in filters employing OTES- and TFS-sepiolites, respectively, with different operational and constructive parameters: (a) Experiment 1: columns 13 cm long ×2 cm diameter; flow velocity 1 m/h; pollutant concentration 5 mg/L; and (b) Experiment 2: 10 cm long × 3 cm diameter; flow velocity 0.6 m/h; pollutant concentration 1 mg/L.

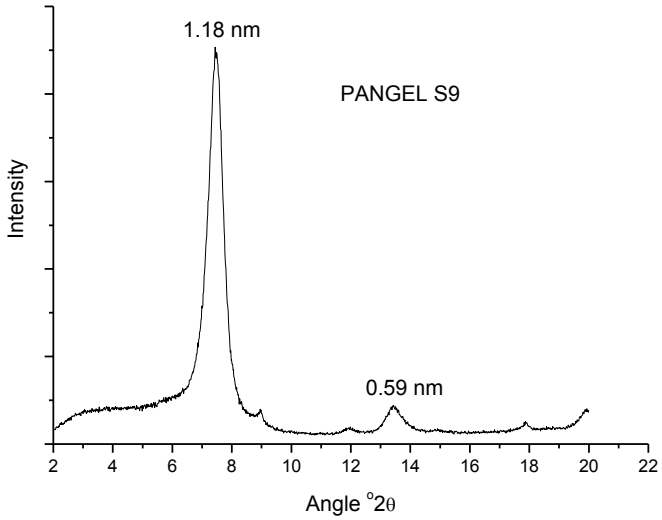

548

549 Figure 1

550

551

552

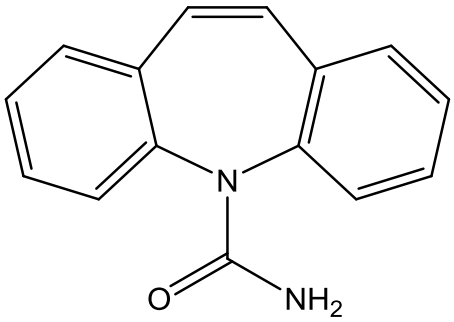

Carbamazepine

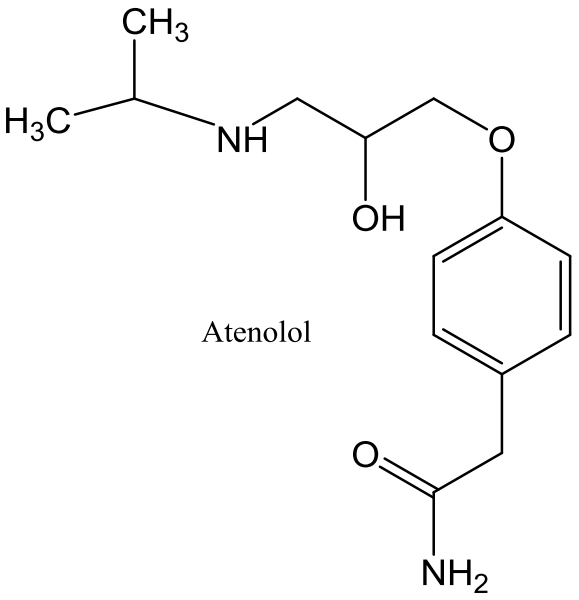

Atenolol

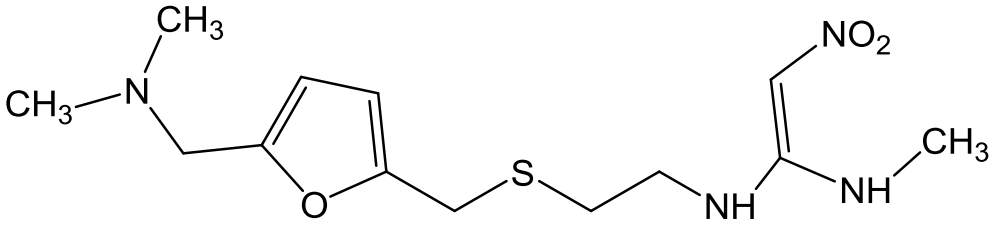

Ranitidine

553

554

555

556 Figure 2

557

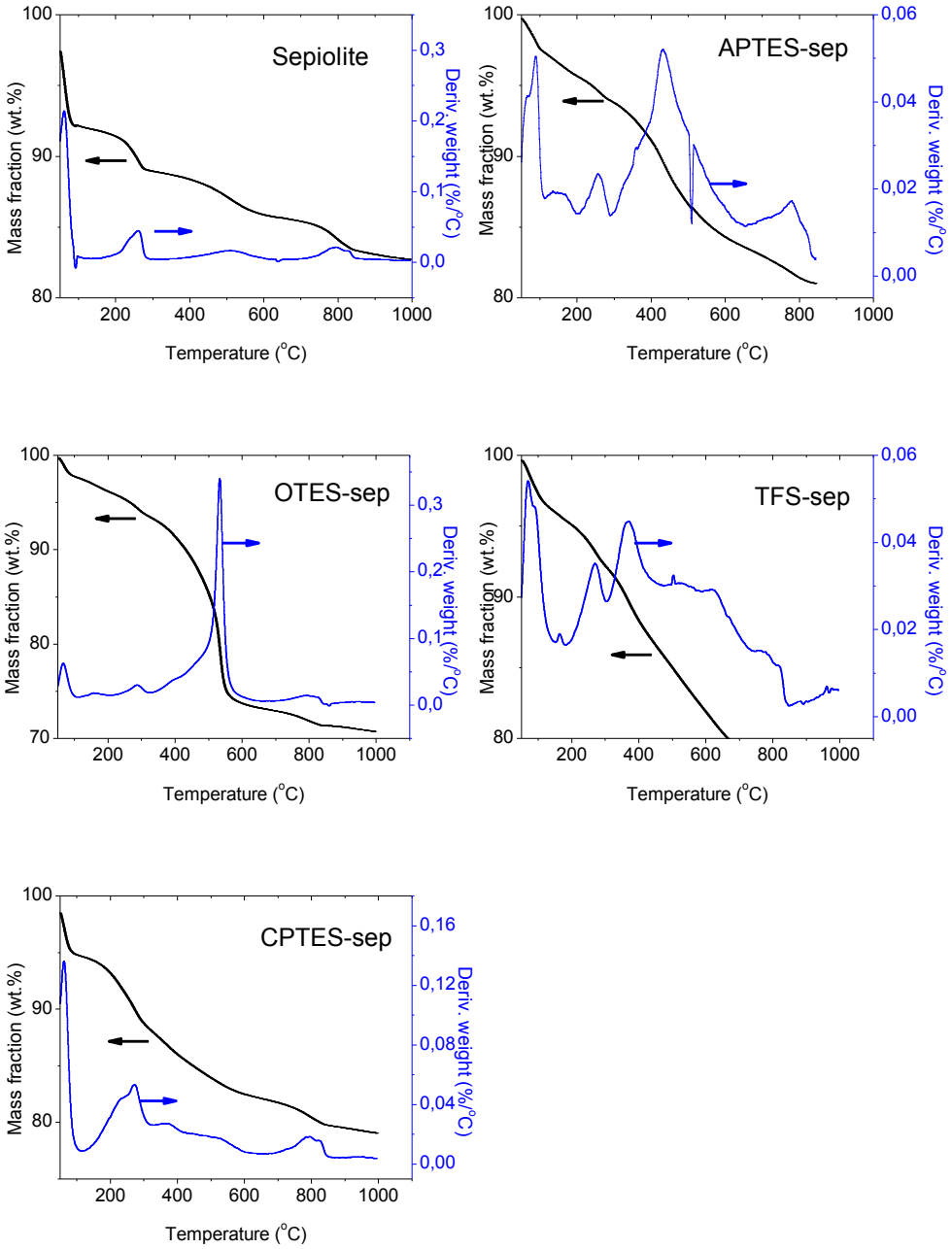

558

559

560 Figure 3

561

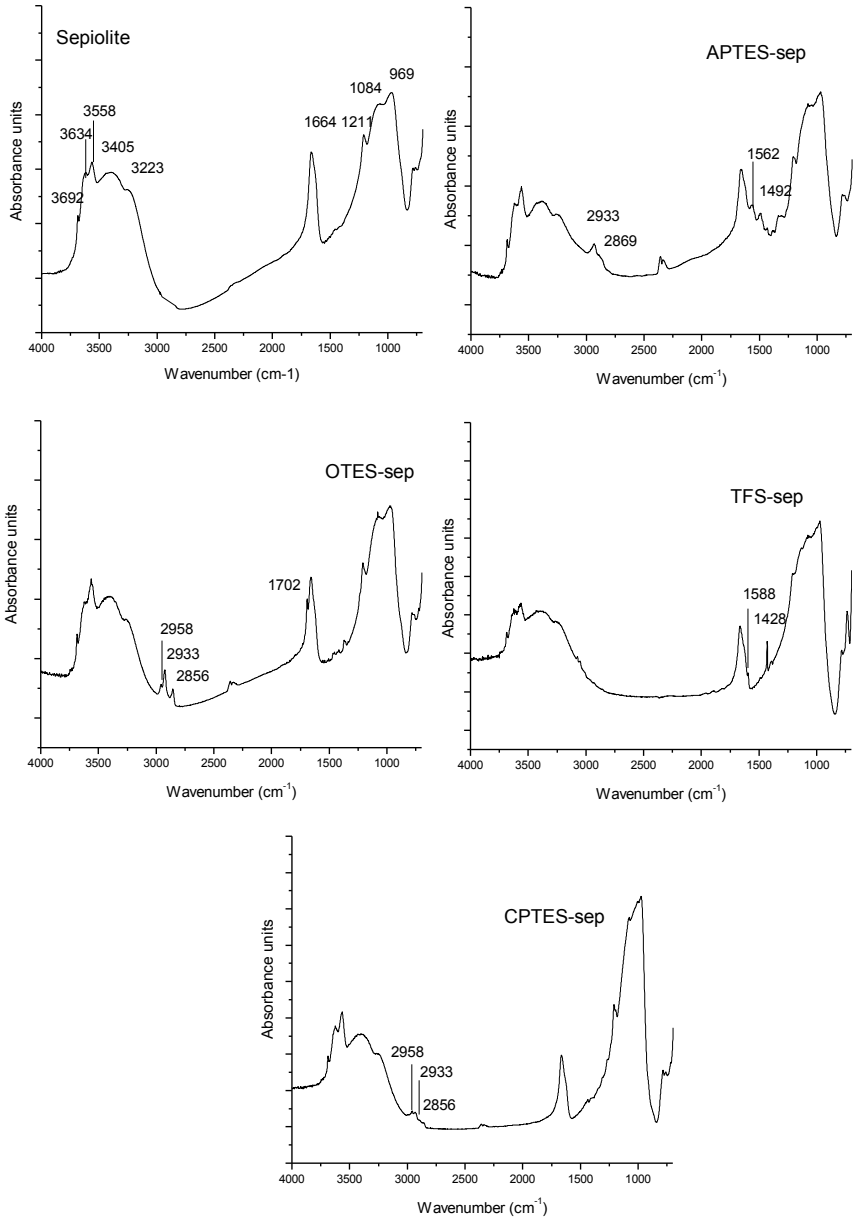

562

563

564 Figure 4

565

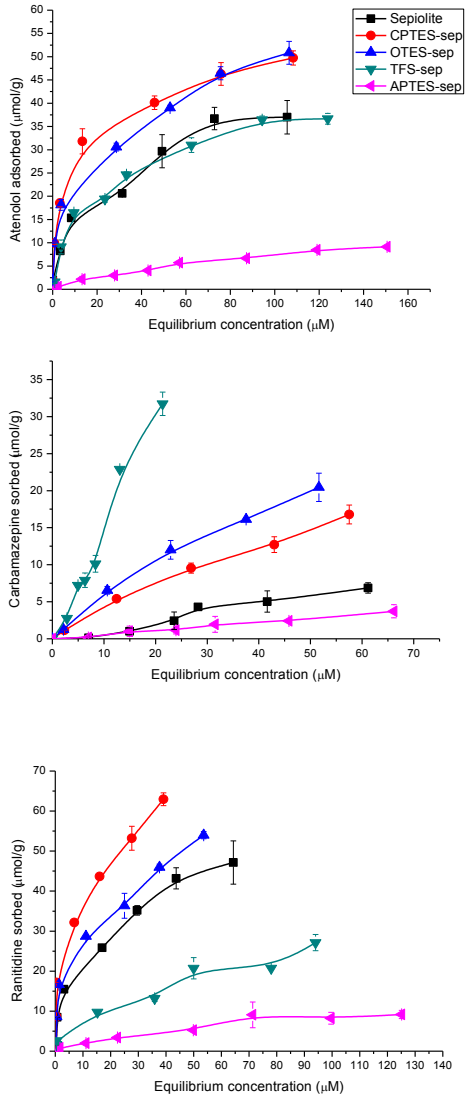
Sepiolite
CPTES-sep
OTES-sep
TFS-sep
APTES-sep
Atenolol adsorbed (μmol/g)
Equilibrium concentration (μM)
Carbamazepine sorbed (μmol/g)
Equilibrium concentration (μM)
Ranitidine sorbed (μmol/g)
Equilibrium concentration (μM)

Figure 5

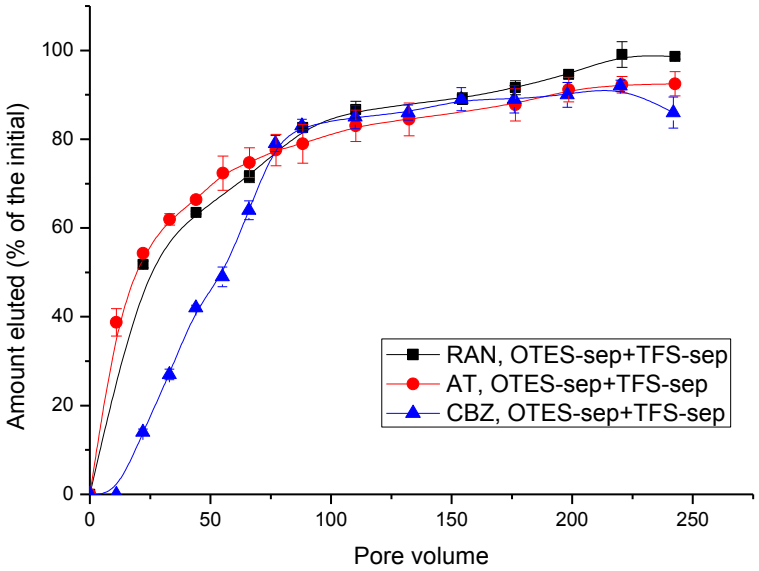

570

571

572 Figure 6

573

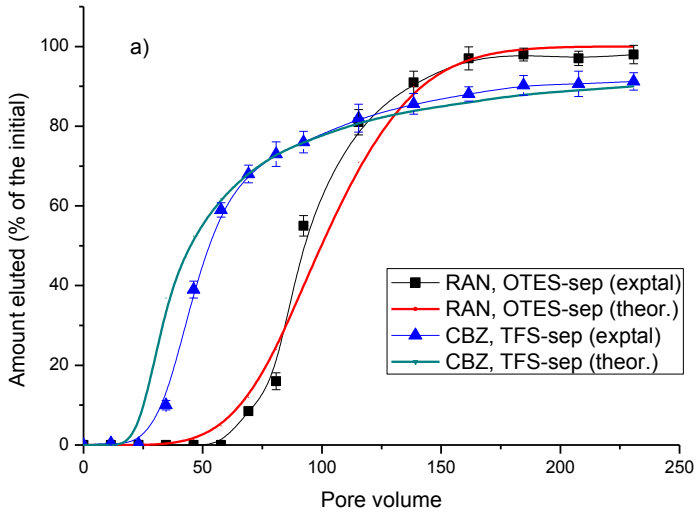

574

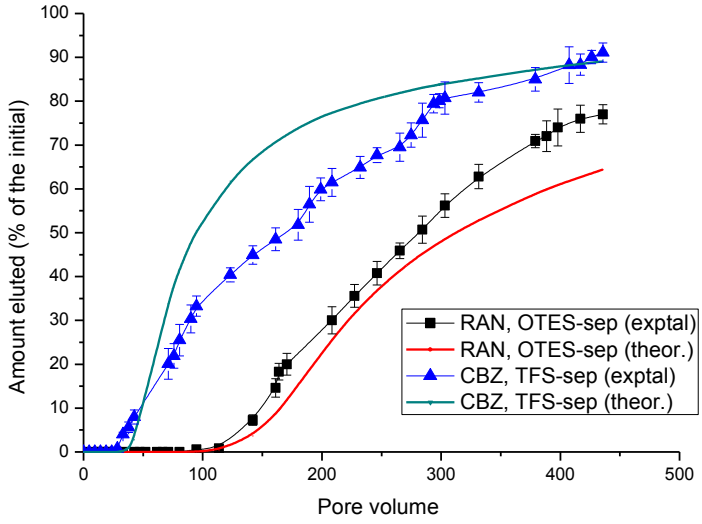

575

576

577 Figure 7

578

579

580

581

582

583

584

585

586

587

588

589

590